Article

JOURNAL OF
REINFORCED
PLASTICS &
COMPOSITES

Journal of Reinforced Plastics and Composites
30(5) 409–415

DOI: 10.1177/0731684410397897
jrp.sagepub.com
SAGE

Approximative formula for post-buckling analysis of non-linearly elastic columns with superellipsoidal cross-sections

Mihael Brojan and Franc Kosel

Abstract

Approximative formulas for post-buckling analysis of non-linearly elastic columns made of Ludwick material are developed for free-clamp, hinge–hinge, and clamp–clamp supports. The columns have a superellipsoidal cross-section. Comparison between analytically obtained and numerical solutions showed good agreement. Additionally, post-buckling configurations for all three types of columns and materials are given in diagrams, from where the influence of material constants on the shape of the deflection curve can be examined.

Keywords

non-linearly elastic column, superellipsoidal cross-section, post-buckling, approximative solution, analytical formula

Introduction

Slender members under sufficient axial compressive loadings may exhibit large lateral displacements which usually lead to sudden failure of structures long before the maximum stresses exceed the limit stress. In designing structures and machines, this phenomenon, called buckling, is thus of major concern. For example, when a straight uniform column is subjected to an axial compression force P, Figure 1(a), it remains straight when P is small and (usually) deflects laterally when P exceeds a certain critical value. This critical value P_{cr} is often named the Euler buckling force.

In this article, buckling and post-buckling of uniform columns which are made of non-linearly elastic material are studied as a continuation of the subject covered by the authors in Ref.[1] In the past few years, similar investigations of geometrically and materially non-linear problems of beam bending have been reported by a number of authors. Contributions that are most closely related to the problem addressed here can be found in Refs.,[2–4] where the mechanical behavior of a cantilever beam made of non-linear Ludwick's bimodulus material is analyzed when subjected to pure bending; and in Ref.[5] where the moment–curvature relation was derived for fibers of superellipsoidal cross-section made of non-linear material for the case of pure bending; and in Refs.,[6,7] where the beam made of functionally graded non-linearly elastic material of Ludwick type is considered.

Boundary conditions and critical loads of the columns investigated in this contribution are listed in Table 1. Critical loads are the solutions of the transcendental equations, $\cos\omega = 0$, $\sin\omega = 0$, and $\omega\sin\omega + 2\cos\omega - 2 = 0$, which can be obtained *via* linearization of the problem.

Formulation of the problem

Let us consider a slender, initially straight column of length L subjected to an axial compression force P, as shown in Figure 1. The column has a cross-section of constant width $2a$ and constant height $2b$

Laboratory for Nonlinear Mechanics, Faculty of Mechanical Engineering, University of Ljubljana, Ljubljana, Slovenia.

Corresponding author:
Mihael Brojan, Laboratory for Nonlinear Mechanics, Faculty of Mechanical Engineering, University of Ljubljana, Askerceva 6, SI-1000 Ljubljana, Slovenia
Email: miha.brojan@fs.uni-lj.si

in the shape of the superellipse (cf. §2.1). The mathematical model of the discussed problem is based on the elastica theory. The material of which the column is made is assumed to be homogenous, incompressible, and isotropic. The non-linear stress–strain relation is given by the Ludwick's formula:

$$\sigma(\varepsilon) = \mathrm{sign}(\varepsilon) E |\varepsilon|^{1/n}, \tag{1}$$

where E and n are material constants.

From static equilibrium of internal forces and inner bending moments which act on an infinitesimal element of the deformed beam, cf. Figure 2, geometrical relations $\mathrm{d}x/\mathrm{d}s = \cos\vartheta$, $\mathrm{d}y/\mathrm{d}s = \sin\vartheta$, from the expression for inner bending moment as a function of normal stress $M = -\int_A \sigma y \mathrm{d}A$, Equation (1), and the normal strain–curvature expression $\varepsilon = -y\rho^{-1}$ and $\rho^{-1} = \mathrm{d}\vartheta/\mathrm{d}s$, we can deduce an equation:

$$EI_{1+n}\frac{1}{n}\left(\frac{\mathrm{d}\vartheta}{\mathrm{d}s}\right)^{(1-n)/n}\frac{\mathrm{d}^2\vartheta}{\mathrm{d}s^2} + P\sin\vartheta + H\sin\vartheta = 0, \tag{2}$$

which together with the accompanying boundary conditions (cf. Table 1) describes the post-buckling behavior of columns subjected to an axial force. Variable s, $0 \le s \le L$, denotes a curvilinear coordinate along the centroidal axis measured from the fixed end of the column and $\vartheta(s)$ represents the angle between the positive direction of the x-axis and the tangent to the centroidal axis at point s.

Remark 1. It should be noted that H and M_0 are the reactive force and moment acting in the upper support of the column, Figure 1(b)–(d). Furthermore, $H,\ M_0 = 0$ for I Euler's case, $H \neq 0,\ M_0 = 0$ for II Euler's case, and $H,\ M_0 \neq 0$ for IV Euler's case.

By introducing quantities:

$$p := \frac{nP}{EI_{1+n}},\ h := \frac{nH}{EI_{1+n}},\ t := p^{n/(1+n)}s, \tag{3}$$

where $t \in [0,\ p^{n/(1+n)}L]$, and introducing parameter η:

$$\eta := \frac{h}{p}, \tag{4}$$

dividing Equation (2) by p, we obtain:

$$\left(\frac{\mathrm{d}\vartheta}{\mathrm{d}t}\right)^{(1-n)/n}\frac{\mathrm{d}^2\vartheta}{\mathrm{d}t^2} + \sin\vartheta + \eta\cos\vartheta = 0. \tag{5}$$

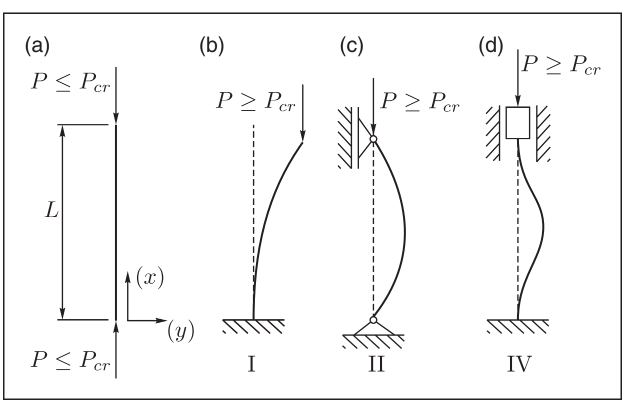

Figure 1. Trivial and post-critical shape modes of I, II, and IV Euler columns.

Superellipse

A generalized ellipse or *superellipse* is a closed curve defined by the following implicit equation:

$$\frac{|z|^\alpha}{a} + \frac{|y|^\beta}{b} = 1, \qquad a, b, \alpha, \beta \in R^+. \tag{6}$$

where a and b are semi-axes. They are special cases of curves which are known in analytical geometry as Lame curves. The name superellipse was proposed by Piet Hein, a Danish poet and scientist who popularized these curves for design purposes.[8]

Remark 2. It can be noted that an ordinary ellipse is obtained if $\alpha = \beta = 2$, and further if $a = b = 1$, the unit circle is obtained. In the limit case $\alpha,\ \beta \to \infty$, Equation (6) yields a superellipse which resembles a rectangle, whereas in the limit case $\alpha,\ \beta \to 0$, it resembles a cross. Some more special cases are depicted in

Table 1. Boundary conditions and critical loads

Euler case	Support	Boundary conditions	$P_{cr} \cdot L^2/(EI)$
I	Clamp-free	$\vartheta(0) = 0,\ \vartheta'(L) = 0$	$\pi^2/4$
II	Hinge–hinge	$\vartheta'(0) = 0,\ \vartheta'(L) = 0$	π^2
IV	Clamp–clamp	$\vartheta(0) = 0,\ \vartheta(L) = 0$	$4\pi^2$

Figure 3, where values of a, b, α, and β are given in parentheses, $(a,\ b,\ \alpha,\ \beta)$.

Superellipse may also be represented parametrically by:

$$\begin{aligned} z =& a\ \mathrm{sign}(\cos\varphi)\,|\cos\varphi|^{2/\alpha} \\ y =& b\ \mathrm{sign}(\sin\varphi)\,|\sin\varphi|^{2/\beta}, \end{aligned}$$

where $\varphi \in [0,\ 2\pi]$. The $1+n$th moment of area can therefore be determined as shown below:

$$\begin{aligned} I_{1+n} :=& \int_A y^{1+n}\mathrm{d}A \\ \overset{\dagger}{=}& -\frac{1}{2+n}\int_{\partial A} y^{2+n}\mathrm{d}z \quad \dagger\text{Green's theorem} \\ =& \frac{8ab^{2+n}}{\alpha(2+n)}\int_0^{\pi/2}(\cos\varphi)^{2/\alpha-1}(\sin\varphi)^{2(2+n)/\beta+1}\mathrm{d}\varphi. \end{aligned}$$

The integral above can be expressed by the Beta function:

$$B(p,\ q) := 2\int_0^{\frac{\pi}{2}}(\cos\varphi)^{2p-1}(\sin\varphi)^{2q-1}\mathrm{d}\varphi, \tag{7}$$

which leads to:

$$I_{1+n} = \frac{4ab^{2+n}}{\alpha(2+n)}B\left(\frac{1}{\alpha},\ \frac{2+n}{\beta}+1\right). \tag{8}$$

Using the identities, cf. Ref.:[9]

$$B(p,\ q) = B(q,\ p), \qquad B(p,\ q+1) = \frac{q}{p+q}B(p,\ q) \tag{9}$$

one can get:

$$I_{1+n} = \frac{4ab^{2+n}}{\alpha(2+n)+\beta}B\left(\frac{1}{\alpha},\ \frac{2+n}{\beta}\right). \tag{10}$$

Remark 3. In the limit case, when $\alpha,\ \beta \to \infty$, it follows:

$$I_{1+n} = \frac{4ab^{2+n}}{2+n}, \tag{11}$$

and further for $n = 1$, a well-known formula $I_2 = 4ab^3/3$ is obtained.

Remark 4. The area of a superellipse $\int_A \mathrm{d}A$ can be obtained by setting $n = -1$ in Equation (10):

$$A = \frac{4ab}{\alpha+\beta}B\left(\frac{1}{\alpha},\ \frac{1}{\beta}\right). \tag{12}$$

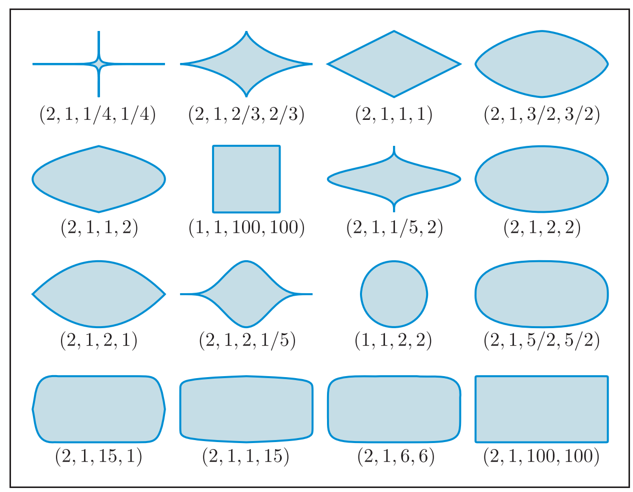

Figure 3. Cross-sections defined by superellipse.

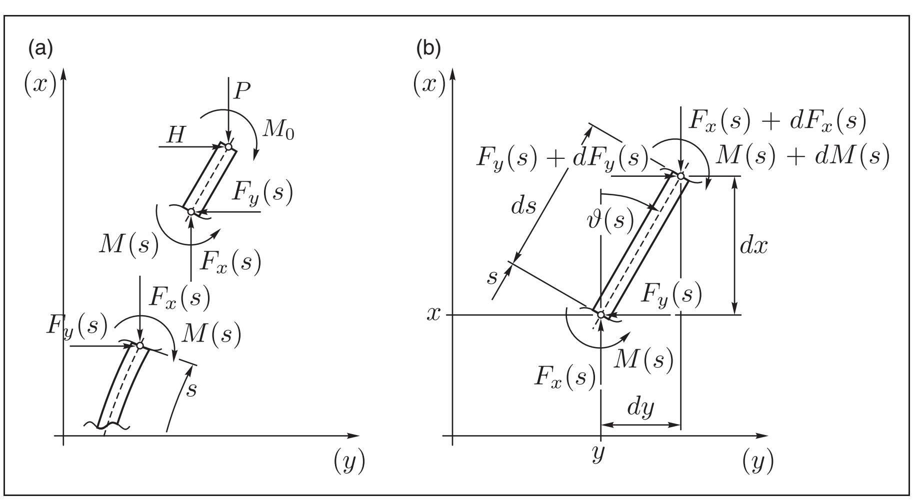

Figure 2. Free body diagram and infinitesimal element of the deflected column.

Determination of the critical force

In immediate post-buckling, $\vartheta(t)$ is expected to be small for all $t \in [0, p^{n/(1+n)}]$. Therefore, approximating $\sin\vartheta \doteq \vartheta$ is reasonable. In the I Euler case, $H \equiv 0$. Then, Equation (5) can be reduced to:

$$\left(\frac{\mathrm{d}\vartheta}{\mathrm{d}t}\right)^{(1-n)/n}\frac{\mathrm{d}^2\vartheta}{\mathrm{d}t^2} + \vartheta = 0. \tag{13}$$

Accompanying boundary conditions are:

$$\vartheta(0) = 0, \qquad \vartheta'\left(p^{n/(1+n)}L\right) = 0. \tag{14}$$

Introducing function u, such that:

$$\vartheta'(t) =: u(\vartheta(t)). \tag{15}$$

and differentiating with respect to variable t give:

$$\vartheta''(t) = u'(\vartheta(t))u(\vartheta(t)). \tag{16}$$

Equation (13) can now be rewritten as:

$$u'u^{1/n} + \vartheta = 0. \tag{17}$$

Integrating and considering Equation (15) yields:

$$\frac{n}{1+n}(\vartheta')^{(1+n)/n} + \frac{\vartheta^2}{2} = c. \tag{18}$$

It follows from the boundary condition $\vartheta'(p^{n/(1+n)}L) = 0$ that:

$$c = \frac{\vartheta_e^2}{2}, \tag{19}$$

where $\vartheta_e := \vartheta(p^{n/(1+n)}L)$. From Equations (18) and (19), one can obtain:

$$\frac{\mathrm{d}\vartheta}{\mathrm{d}t} = \left(\frac{1+n}{n}\right)^{n/(1+n)}\left(\frac{1}{2}\right)^{n/(1+n)}\left(\vartheta_e^2 - \vartheta^2\right)^{n/(1+n)}. \tag{20}$$

Rewriting the above equation and integrating over the domains of ϑ and t on each side of the equation lead to:

$$\int_{\vartheta(0)}^{\vartheta\left(p^{n/(1+n)}L\right)} \frac{\mathrm{d}\vartheta}{\left(\vartheta_e^2 - \vartheta^2\right)^{n/(1+n)}} = \int_0^{p^{n/(1+n)}L}\left(\frac{1+n}{n}\right)^{n/(1+n)}\left(\frac{1}{2}\right)^{n/(1+n)}\mathrm{d}t. \tag{21}$$

The integral on the RHS is equal to:

$$S_{\mathrm{RHS}} = \left(\frac{1+n}{n}\right)^{n/(1+n)}\left(\frac{1}{2}\right)^{n/(1+n)} p^{n/(1+n)}L. \tag{22}$$

As already mentioned, $\vartheta(t)$ is expected to be small at immediate post-buckling and it is therefore reasonable to linearize function ϑ, so that:

$$\vartheta(t) \doteq \vartheta_e p^{-n/(1+n)}L^{-1}t. \tag{23}$$

Taking this into account, the integral on LHS can be written as:

$$S_{\mathrm{LHS}} = \frac{\vartheta_e^{(1-n)/(1+n)}}{p^{n/(1+n)}L}\int_0^{p^{n/(1+n)}L}\frac{\mathrm{d}t}{\left(1 - p^{-2n/(1+n)}L^{-2}t^2\right)^{n/(1+n)}}. \tag{24}$$

Introducing variable $w = p^{-2n/(1+n)}L^{-2}t^2$:

$$S_{\mathrm{LHS}} = \frac{\vartheta_e^{(1-n)/(1+n)}}{2}\int_0^1 w^{-1/2}(1-w)^{-n/(1+n)}\mathrm{d}w. \tag{25}$$

Beta function B, given by Equation (7), can also be written in the following form, Ref.:[9]

$$B(p,\ q) = \int_0^1 x^{p-1}(1-x)^{q-1}\mathrm{d}x. \tag{26}$$

Hence:

$$S_{\mathrm{LHS}} = \frac{\vartheta_e^{(1-n)/(1+n)}}{2}B\left(\frac{1}{2},\ \frac{1}{1+n}\right). \tag{27}$$

Equating (27) and (22) results in:

$$p(n) = \frac{n\vartheta_e^{(1-n)/n}}{2^{1/n}(1+n)L^{(1+n)/n}}B\left(\frac{1}{2},\ \frac{1}{1+n}\right)^{(1+n)/n} \tag{28}$$

and:

$$P_{\mathrm{I}}(n) = \frac{\vartheta_e^{(1-n)/n}EI_{1+n}}{2^{1/n}(1+n)L^{(1+n)/n}}B\left(\frac{1}{2},\ \frac{1}{1+n}\right)^{(1+n)/n}. \tag{29}$$

which follows from $(3)_2$ additionally.

Approximative formula for post-buckling behavior analysis of non-linearly elastic columns with super-ellipsoidal cross-sections is therefore:

$$P_{\mathrm{I}}(n) = \frac{2^{(2n-1)/n}E\vartheta_e^{(1-n)/n}ab^{2+n}}{(1+n)(\alpha(2+n)+\beta)L^{(1+n)/n}} B\left(\frac{1}{\alpha},\ \frac{2+n}{\beta}\right)B\left(\frac{1}{2},\ \frac{1}{1+n}\right)^{(1+n)/n}. \tag{30}$$

The critical force P_{cr} for the linearly elastic column can be found by setting $n = 1$:

$$P_{\mathrm{I,\,cr}} = EI_2\frac{\pi^2}{4L^2}. \tag{31}$$

Expression for $P_{\mathrm{II}}(n)$ can be derived in a similar way, namely, considering obvious natural symmetry in the deflection curve of II Euler case, the first boundary condition in (14) can be replaced by $\vartheta\left(p^{n/(1+n)}L/2\right) = 0$. Thus, an equation, equivalent to Equation (21), can be written $2\int_{\vartheta(p^{n/(1+n)}L)}^{\vartheta(p^{n/(1+n)}L/2)} \ldots = 2\int_{p^{n/(1+n)}L}^{p^{n/(1+n)}L/2} \ldots$ Parameter $\vartheta_e := \vartheta(p^{n/(1+n)}L)$ and approximation $\vartheta \doteq \vartheta_e(2/(p^{n/(1+n)}L)t - 1)$ are used to get the following expressions:

$$P_{\mathrm{II}}(n) = \frac{2\vartheta_e^{(1-n)/n} EI_{1+n}}{(1+n)L^{(1+n)/n}} B\left(\frac{1}{2}, \frac{1}{1+n}\right)^{(1+n)/n}, \tag{32}$$

$$P_{\mathrm{II}}(n) = \frac{2^3 E\vartheta_e^{(1-n)/n} ab^{2+n}}{(1+n)(\alpha(2+n)+\beta)L^{(1+n)/n}} B\left(\frac{1}{\alpha}, \frac{2+n}{\beta}\right) B\left(\frac{1}{2}, \frac{1}{1+n}\right)^{(1+n)/n}, \tag{33}$$

from where:

$$P_{\mathrm{II,cr}} = EI_2 \frac{\pi^2}{L^2}. \tag{34}$$

arises in the case of $n = 1$.

From double natural symmetry in the deflection curve of IV Euler case, an expression for $P_{\mathrm{VI}}(n)$ can be derived. In this case, the second boundary condition is replaced by $\vartheta'\left(p^{n/(1+n)}L/4\right) = 0$. An equation, equivalent to Equation (21), can now be written $4\int_0^{\vartheta(p^{n/(1+n)}L/4)} \ldots = 4\int_0^{p^{n/(1+n)}L/4} \ldots$ Parameter ϑ_e and approximation for ϑ are now $\vartheta_e := \vartheta(p^{n/(1+n)}L/4)$ and $\vartheta \doteq (4\vartheta_e/x)t$. Thus:

$$P_{\mathrm{IV}}(n) = \frac{2^{(1+2n)/n}\vartheta_e^{(1-n)/n} EI_{1+n}}{(1+n)L^{(1+n)/n}} B\left(\frac{1}{2}, \frac{1}{1+n}\right)^{(1+n)/n}, \tag{35}$$

$$P_{\mathrm{IV}}(n) = \frac{2^{(1+4n)/n} E\vartheta_e^{(1-n)/n} ab^{2+n}}{(1+n)(\alpha(2+n)+\beta)L^{(1+n)/n}} B\left(\frac{1}{\alpha}, \frac{2+n}{\beta}\right) B\left(\frac{1}{2}, \frac{1}{1+n}\right)^{(1+n)/n}, \tag{36}$$

and for $n = 1$

$$P_{\mathrm{IV,cr}} = EI_2 \frac{4\pi^2}{L^2}. \tag{37}$$

Remark 5. The results represented by Equations (31), (34), and (37) are identical to well-known formulas found in the literature, Ref.[10]

Examples

In this section, we show a comparison between the results obtained from the formulas (30), (33), and (36) we constituted and numerical solutions which were obtained by applying the Runge–Kutta–Fehlberg integration and shooting method. Additionally, post-buckling configurations for all three types of columns and materials ($n < 1$, $n = 1$, $n > 1$) are given for illustration.

I Euler case

Post-buckling force P as a function of angle of rotation $\vartheta_e = \vartheta(L)$ is shown in Figure 4 for a free-clamp supported column. The results of numerical and analytical calculations are in good agreement even at relatively large angles of rotation. Namely, at $\vartheta_e = 0.285$, $\vartheta_e = 0.518$, $\vartheta_e = 0.701$, and $\vartheta_e = 1.030$, the differences between numerically and analytically calculated values of post-buckling force in the $n = 2$ case are 1.1%, 3.5%, 6.4%, and 13.6%, respectively. In the case of $n = 0.6$, there are differences of 1.1%, 3.2%, 6.4%, and 12.1% at $\vartheta_e = 0.296$, $\vartheta_e = 0.517$ $\vartheta_e = 0.735$, and $\vartheta_e = 1.021$, respectively.

Figure 5 illustrates the results calculated from the analytical formula (30). It shows the post-buckling load as a function of angle ϑ_e for $n = 0.6$ for different shapes of the cross-section. It should be emphasized that these results arise from one formula only, cf. (30).

The influence of material constant n on post-buckling configurations for a free-clamp supported column is depicted in Figure 6. The diagrams are displayed at constant values of $\vartheta_e = 0.5$, $\vartheta_e = 1.0$, $\vartheta_e = 2.0$, and $\vartheta_e = 3.0$.

II Euler case

Results comparable to those in the previous case are obtained for a hinge–hinge supported column, Figure 7. The difference between post-buckling loads calculated *via* numerical and analytical approaches are 1.3%, 3.2%, 6.4%, and 13.6% at $\vartheta_e = 0.308$, $\vartheta_e = 0.495$, $\vartheta_e = 0.701$, and $\vartheta_e = 1.030$, respectively

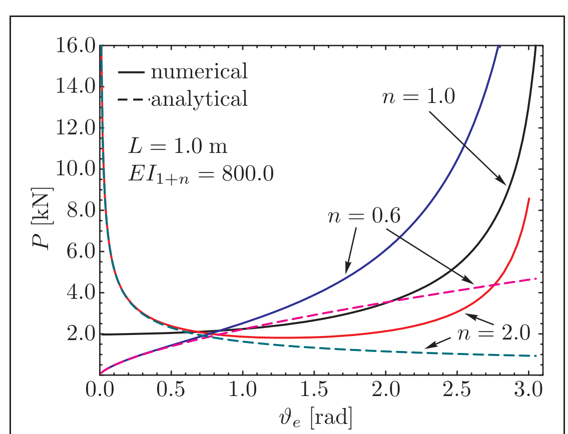

Figure 4. Comparison between analytical and numerical solutions.

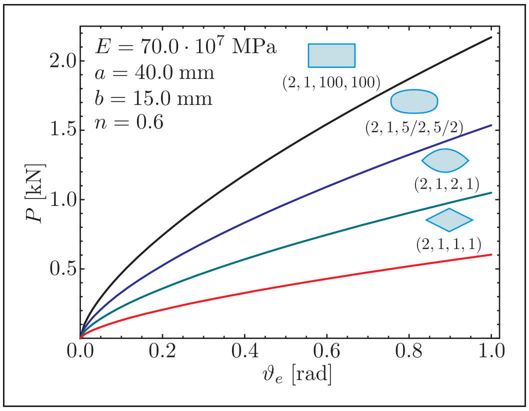

Figure 5. Post-buckling load as a function of the angle of rotation ϑ_e.

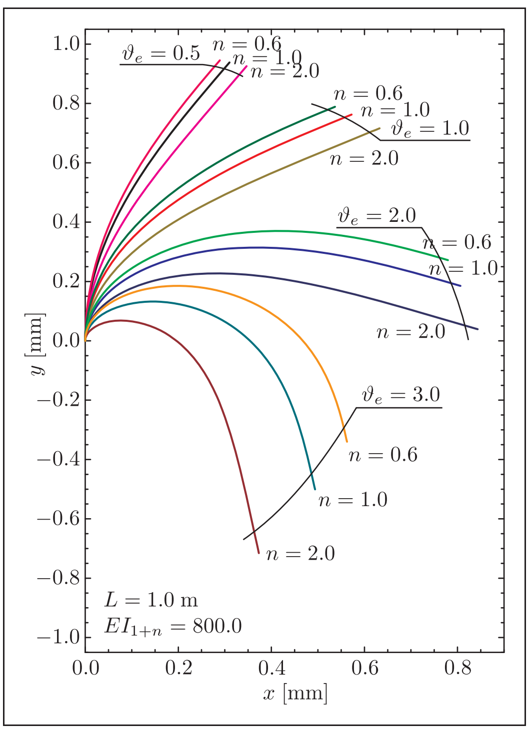

Figure 6. Post-buckling configurations for free-clamp supported column.

for $n = 2$. For $n = 0.6$, there are differences of 1.1%, 3.2%, 5.8%, and 12.1% at $\vartheta_e = 0.296$, $\vartheta_e = 0.517$, $\vartheta_e = 0.699$, and $\vartheta_e = 1.021$, respectively.

A similar influence of material constant n on post-buckling configurations is also noticeable in the case of hinge–hinge supported column, Figure 8.

IV Euler case

As expected, the results obtained for a clamp–clamp supported column are comparable to those in both previous cases, Figure 9. The difference between

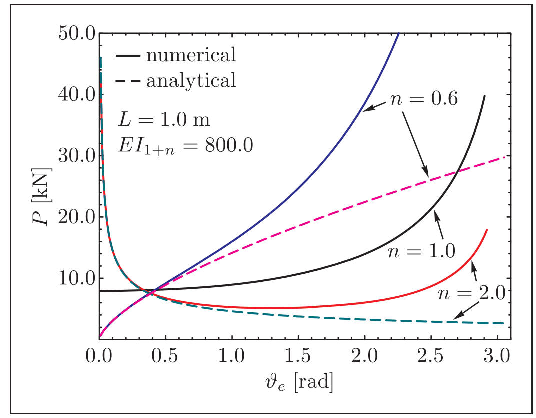

Figure 7. Comparison between analytical and numerical solutions.

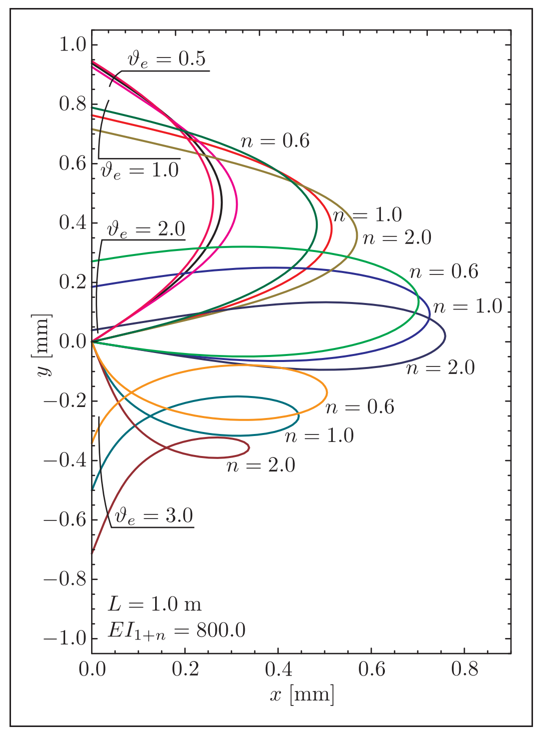

Figure 8. Post-buckling configurations for hinge–hinge supported column.

post-buckling loads calculated *via* numerical and analytical approaches are in this case 1.2%, 3.7%, 6.4%, and 13.6% at $\vartheta_e = 0.296$, $\vartheta_e = 0.530$, $\vartheta_e = 0.701$, and $\vartheta_e = 1.030$, respectively for $n = 2$. For $n = 0.6$, there are differences of 1.3%, 3.1%, 6.4%, and 11.7% at $\vartheta_e = 0.342$, $\vartheta_e = 0.507$, $\vartheta_e = 0.735$, and $\vartheta_e = 1.0$, respectively. In this case, $\vartheta_e = \vartheta(L/4)$.

Post-buckling configurations in correlation with the influence of material constant n on deformation for a clamp–clamp supported column can be found in Figure 10.

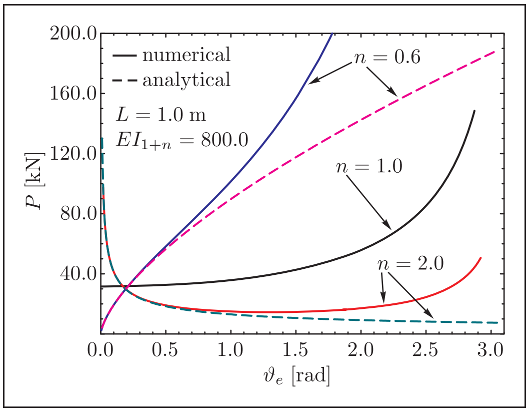

Figure 9. Comparison between analytical and numerical solutions.

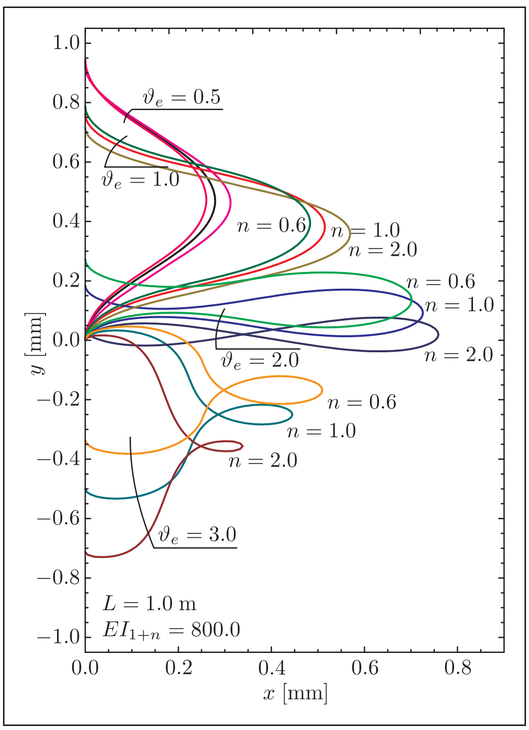

Figure 10. Post-buckling configurations for clamp–clamp supported column.

Conclusion

The problems which involve geometrically exact mechanics, for example, post-buckling analysis of columns are usually difficult to solve. Since analytical solutions are quite rare one has to rely on finding the solution numerically, which can be quite time consuming. The results of this article are useful in engineering practice when analyzing post-buckling behavior of non-linearly elastic columns, e.g., made from rubber. Relatively simple analytical formulas are constituted for free-clamp, hinge–hinge, and clamp–clamp supports of columns which have super-ellipsoidal cross-sections and can therefore be of an arbitrary shape between an ellipse and a rectangle. The accuracy of the analytical formula has been validated numerically, applying the Runge–Kutta–Fehlberg integration and shooting method. A good agreement between the numerical and analytical approaches has been confirmed for relatively large angles of rotation for all three types of supports discussed. Additionally, post-buckling configurations for all three types of columns and materials ($n < 1$, $n = 1$, $n > 1$) are given for illustration. The diagrams from which the influence of material constant n on the shape of the deflection curve can be examined are displayed at four constant values of angle ϑ_e.

Funding

This research received no specific grant from any funding agency in the public, commercial, or not-for-profit sectors.

References

1. Brojan M, Puksic A and Kosel F. Buckling and post-buckling of a nonlinearly elastic column. *Z Angew Math Mech* 2007; 87(7): 518–527.
2. Baykara C, Guven U and Bayer I. Large deflections of a cantilever beam of nonlinear bimodulus material subjected to an end moment. *J Reinf Plast Compos* 2005; 24(12): 1321–1326.
3. Brojan M, Videnic T and Kosel F. Non-prismatic non-linearly elastic cantilever beams subjected to an end moment. *J Reinf Plast Compos* 2007; 26(11): 1071–1082.
4. Shatnawi AS and Al-Sadder S. Exact large deflection analysis of non-prismatic cantilever beams of nonlinear bimodulus material subjected to tip moment. *J Reinf Plast Compos* 2007; 26(12): 1253–1268.
5. Lee KW. Bending analysis of nonlinear material fibers with a generalized elliptical cross-section. *Text Res J* 2005; 75(10): 710–714.
6. Kang YA and Li XF. Bending of functionally graded cantilever beam with power-law non-linearity subjected to an end force. *Int J Nonlinear Mech* 2009; 44(6): 696–703.
7. Kang YA and Li XF. Large deflections of a non-linear cantilever functionally graded beam. *J Reinf Plast Compos* 2010; 29(12): 1761–1774.
8. Jaklic A, Leonardis A and Solina F. Superquadrics and their geometric properties. In: Borgefors G, Deriche R, Huang ThS, Ikeuchi K, Jiang T, Klette R, et al. (eds) *Segmentation and recovery of superquadrics*. Chap. 2. In series Computational imaging and vision. Dordrecht: Kluwer Academic Publishers, 2000, pp.13–39.
9. Bell WW. *Special functions for scientists and engineers*. New York: Dover Publications, 2004.
10. Wang CM, Wang CY and Reddy JN. *Exact solutions for buckling of structural members*. Boca Raton, FL: CRC Press, 2005.